Available online at www.sciencedirect.com
ScienceDirect
International Journal of Heat and Mass Transfer 51 (2008) 2482–2493
International Journal of HEAT and MASS TRANSFER
www.elsevier.com/locate/ijhmt

Experimental and theoretical studies on subcooled flow boiling of pure liquids and multicomponent mixtures

M. Jamialahmadi [a], H. Müller-Steinhagen [b,c,*], H. Abdollahi [a], A. Shariati [a]

[a] The University of Petroleum Industry, Ahwaz, Iran
[b] Institute of Technical Thermodynamics, German Aerospace Center, Germany
[c] Institute of Thermodynamics and Thermal Engineering, University of Stuttgart, Germany

Received 16 April 2007; received in revised form 25 July 2007
Available online 22 October 2007

Abstract

To improve the design of modern industrial reboilers, accurate knowledge of boiling heat transfer coefficients is essential. In this study flow boiling heat transfer coefficients for binary and ternary mixtures of acetone, isopropanol and water were measured over a wide range of heat flux, subcooling, flow velocity and composition. The measurements cover the regimes of convective heat transfer, transitional boiling and fully developed subcooled flow boiling. Two models are presented for the prediction of flow boiling heat transfer coefficients. The first model is the combination of the Chen model with the Gorenflo correlation and the Schlünder model for single and multicomponent boiling, respectively. This model predicts flow boiling heat transfer coefficients with acceptable accuracy, but fails to predict the nucleate boiling fraction NBF reasonably well. The second model is based on the asymptotic addition of forced convective and nucleate boiling heat transfer coefficients. The benefit of this model is a further improvement in the accuracy of flow boiling heat transfer coefficient over the Chen type model, simplicity and the more realistic prediction of the nucleate boiling fraction NBF.
© 2007 Elsevier Ltd. All rights reserved.

1. Introduction

Boiling heat transfer to pure liquids and liquid mixtures occurs most commonly in evaporators throughout the process industry for chemical, petrochemical and hydrometallurgical operations. Their duty is to evaporate the process liquid at the bottom of distillation and absorption columns to supply the energy required for the separation. The process fluid enters the evaporator at a temperature which is lower than its saturation temperature. When the heat flux from the heating surface to the process fluid is increased above a certain value, the convective heat transfer is not enough to prevent the wall temperature from rising above the saturation temperature of the flowing liquid. The elevated wall temperature superheats the liquid in contact with the wall and activates nucleation sites, thus generating vapor bubbles at the heat transfer surface. These bubbles condense in the colder liquid away from the heat transfer resulting thus in no net vapor production. At high heat fluxes the onset of subcooled boiling is already encountered at high degree of subcooling and the vapor bubbles may grow and collapse while still attached to or even sliding along the heat transfer surface. At first, nucleation occurs only in patches along the heated surface while forced convection persists in between. As the heat flux is increased more nucleation sites are activated until at fully developed nucleate boiling the complete surface is covered by bubbles. According to Wenzel [1], subcooled boiling can occur over a considerable length of the evaporator and may represent up to 50% of the total heat duty.

During flow boiling heat is transferred from the heated surface to the liquid by several mechanisms [2]:

1. Heat transport by the latent heat of evaporation. This mechanism is important at high pressures but negligible at normal pressure [3].

* Corresponding author. Address: Institute of Thermodynamics and Thermal Engineering, University of Stuttgart, Germany. Tel.: +49 71168563536; fax: +49 71168563503.
E-mail address: hms@itw.uni-stuttgart.de (H. Müller-Steinhagen).

0017-9310/$ - see front matter © 2007 Elsevier Ltd. All rights reserved.
doi:10.1016/j.ijheatmasstransfer.2007.07.052

Nomenclature

a_{ij}	binary constant
Bo	boiling number
d_h	hydraulic diameter (m)
f_i	fanning friction number
F	enhancement factor
F_p	parameter
Gr	Grashof number
h	enthalpy (J/kg)
Δh_v	heat of evaporation (J/kg)
l_{th}	heated length (m)
L	heater length (m)
ΔL	defined by Eq. (14)
$\dot{m}$	mass flux (kg/m^2 s)
NBF	nucleate boiling fraction
Nu	Nusselt number
Pe	Peclet number
Ph	phase change number
P_r	reduced pressure
Pr	Prandtl number
$\dot{q}$	heat flux (W/m^2)
$\dot{q}_0$	reference heat flux (W/m^2)
r	radius (m)
r^*	radius ratio for annulus
Re	Reynolds number
R_p	surface roughness (μm)
s	distance between thermocouple location and heat transfer surface (m)
S	suppression factor
T	temperature (K)
x	mole fraction
$\dot{x}$	vapor mass fraction
X_{tt}	Martinelli parameter
V	molar volume (cm^3/mol)
y	vapor phase mole fraction

Greek symbols

Λ	Wilson constant
α	heat transfer coefficient (W/m^2 K)
α_0	reference heat transfer coefficient (W/m^2 K)
β	mass transfer coefficient (m/s)
γ	activity coefficient
λ	thermal conductivity (W/m K)
μ	viscosity (kg/ms)
ρ	density (kg/m^3)
θ	the ratio of Prandtl numbers at bulk and wall temperatures

Subscripts–superscripts

b	bulk
fp	flow boiling
fc	forced convective
i	inner
id	ideal
l	liquid
lam	laminar
o	outer
pb	pool boiling
ph	interface
sat	saturation
th	thermocouple
tp	two phase
turb	turbulent
v	vapor
w	wall
∞	fully developed

2. Heat transport by continuous evaporation at the root and condensation at the top of the bubbles, while the bubbles are still attached to the heat transfer surface. This mechanism is also very important for fouling of the heat transfer surface when the process fluid is contaminated [4].
3. Unsteady state heat transfer caused by bubble agitation of the thermal boundary layer adjacent to the heat transfer surface.
4. Heat transfer by single phase convection between the bubble growth zones.

Over the last decades, extensive experimental and theoretical research efforts have been devoted to the understanding of the fundamental aspects of nucleate and saturated flow boiling of pure liquids and of liquid mixtures. The results of these investigations have been documented and critically discussed in several review papers, e.g. Steiner and Taborek [5], Thome [6], Kandlikar [7], Stephan [8], and Cheng and Mewes [9]. Steiner and Taborek [5] summarized the various available correlations for the prediction of saturated flow boiling. They concluded that most of the correlations may reproduce the data in the middle ranges of operating parameters, but will fail as extreme conditions are approached. Thome [6] reviewed the research on pool boiling and flow boiling of refrigerants and addressed several key points on flow boiling of mixtures. Kandlikar [7] performed a historical review on modeling flow boiling of binary mixtures and presented a summary of several important available correlations for binary mixtures. Stephan [8], in his review paper, analyzed the mechanisms of heat transfer for flow boiling of mixtures, and explained the reasons for the reduction of heat transfer coefficient of mixtures in comparison to pure liquids with the same physical properties as the mixtures. Most recently, Cheng and Mewes [9] presented a

state-of-the-art review on this important area and identified what has been done so far and what still needs to be done in the future. The general conclusions of these review papers are that the available fundamental information on flow boiling is rather scarce and that thorough understanding of the flow boiling mechanisms is required to improve operation and design of modern industrial reboilers.

Even though substantial efforts have been devoted so far to clarify the boiling phenomena and to correlate the experimental data for heat transfer during boiling of pure liquids and liquid mixtures, the results have not been satisfactory because of the complexity and the poor reproducibility of the underlying phenomena. This may be due to the fact that, in addition to the thermo-physical properties of the fluid, many parameters such as surface condition, mass transfer effect, presence of impurities and deposition of foreign materials on the heat transfer surface are inherent factors that influence bubble generation. Even though the general shape of the characteristic boiling curve is known for various combinations of liquid and surface conditions, there is still considerable disagreement about the exact shape and location of the curves. The principal aim of the present investigation is, therefore, to measure subcooled flow boiling heat transfer of single and multicomponent mixtures over a wide range of fluid velocities, heat fluxes, compositions and subcooled temperatures. New experimental results are presented for fluid velocities higher than 0.5 m/s, a region where no data have been available in the literature. Two predictive models are presented; the first model is a linear addition of the forced convective and boiling heat transfer coefficients according to Chen [10], while the second model is based on the asymptotic addition of the two coefficients. Both models cover prediction of heat transfer coefficients from the convective regime up to the fully developed boiling regime for single component fluids and multicomponent mixtures under saturated and subcooled flow boiling conditions.

2. Experimental equipment and procedure

2.1. Experimental equipment

Fig. 1 shows the test apparatus used for the present investigations. The liquid flows in a closed loop consisting of temperature controlled storage tank, pump and test section. The flow velocity of the fluid was measured with calibrated orifice plates. The fluid temperature was measured by thermocouples located in two mixing chambers, before and after the test section. The complete rig was made from stainless steel. Thermocouple voltages, the voltage signal from the flow meter, current and voltage drop from the test heater were all measured and processed with a data acquisition system in conjunction with temperature controller and variac. The test section shown in Fig. 2 consists of an electrically heated cylindrical rod with a stainless steel surface, which is mounted concentrically within the surrounding pipe. The dimensions of the test section are: diameter of heating rod, 10.67 mm; annular gap, 14.73 mm; length of heating rod, 400 mm; length of heated section, 99.1 mm. Heat fluxes and wall temperatures can be as high as 450,000 W/m^2 and 270 °C, respectively. This heater has been manufactured by Ashland Chemical

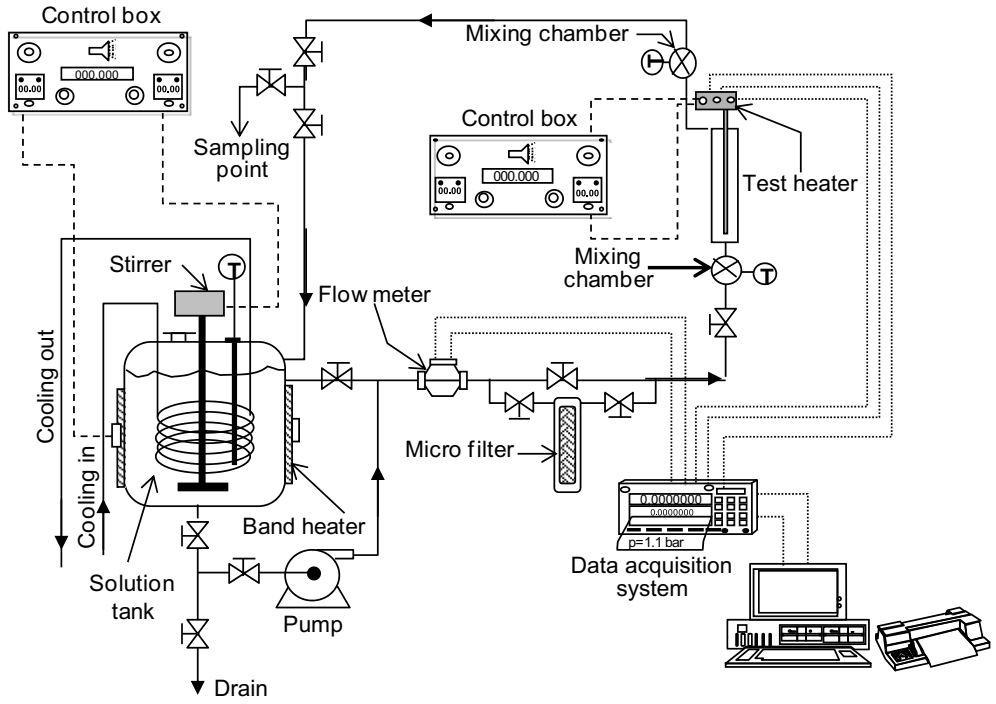

Fig. 1. Schematic drawing of the experimental apparatus.

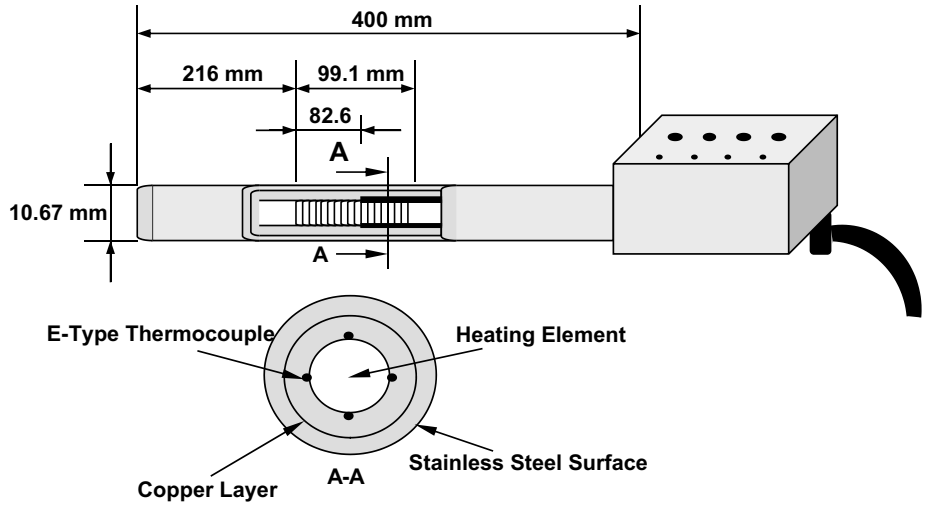

Fig. 2. Schematic drawing of the test heater.

Company according to an HTRI design. The local wall temperatures have been measured with four stainless steel sheathed miniature thermocouples which have been installed close to the heat transfer surface. The temperature drop between the thermocouple location and the heat transfer surface can be calculated from:

$$T_w = T_{th} - \dot{q}\frac{s}{\lambda_w} \tag{1}$$

The ratio between the distance of the thermocouples from the surface and the thermal conductivity of the tube material (s/λ_w) was determined for each thermocouple by calibration measurements using a Wilson plot technique [11]. A typical value of s/λ_w was 0.14 m^2 K/kW. The average temperature difference for each test section was the arithmetic average for the four thermocouple locations around the tube/rod circumference. The average of 10 subsequent voltage readings was used to determine the difference between the wall and bulk temperature for each thermocouple. The local heat transfer coefficient α is then calculated from:

$$\alpha = \frac{\dot{q}}{T_w - T_b} \tag{2}$$

The accuracy of the calibration was checked by comparing the experiments with the predictions of the Gnielinski [12] equation for heat transfer during turbulent flow in pipes and annuli. Agreement was better than ±5%. All measurements were performed with decreasing heat flux to eliminate hysteresis effects due to inactivated bubble nucleation sites (Müller-Steinhagen et al. [13]).

Acetone, isopropanol, distilled water, as well as binary and ternary mixtures of these components are used as test liquids because the physical properties of these components are well known. This guarantees that the calculation error during correlating and modeling of the experimental data are minimized. The vapor–liquid equilibrium required for the calculation of pool boiling heat transfer coefficients of mixtures can be estimated using the Antoine equation for the vapor pressure and the Wilson equation for the activity coefficient, according to Eqs. (3)–(5):

$$y_{i,ph} = \frac{\gamma_i P_i^{sat}}{P} x_{i,ph} \tag{3}$$

where

$$\gamma_i = \exp\left[1 - \ln\left(\sum_j x_j \Lambda_{ij}\right) - \sum_k \frac{x_k}{x_k \Lambda_{kj}}\right] \tag{4}$$

and

$$\Lambda_{ij} = \frac{V_j}{V_i}\exp\left(-\frac{a_{ij}}{RT}\right) \tag{5}$$

Heat transfer coefficients have been recorded only after steady state was reached for the chosen system parameters. The fluid composition was measured before and after each run with a gas chromatograph or by density meter. Some runs were repeated later to check the reproducibility of the experiments, which proved to be excellent. The range of the experimental parameters is given in Table 1.

2.2. Error analysis

The experimental error for the measured heat transfer coefficients may be due to errors in the measurement of heat flux, bulk and heat transfer surface temperature. As all test heaters were sanded with grade 240 emery paper, it was postulated that in all experiments the heat transfer

Table 1
Range of operating parameters

Flow velocity	$0.3 \leqslant v \leqslant 3$ m/s
Heat flux	$15 \leqslant q \leqslant 400$ kW/m^2
Concentration	0–1 mole fraction
Bulk temperature	$80 \leqslant T_b \leqslant 98$ °C
Surface temperature	$100 \leqslant T_w \leqslant 170$ °C

surfaces were comparable with respect to surface roughness. By repeating several tests the same results were obtained, which confirms the above assumption. The error of the adjusted heat flux is due to errors in the measurements of electrical current and voltage. The power delivered by the heater box showed small fluctuations which create a maximum error of about 1.1% of the target value. It is accepted that this phenomenon has some minor effect on the values of the heat transfer coefficient. The liquid and vapor temperatures were measured with K-type thermocouples located in the bulk of the solution. These thermocouples were initially calibrated against a quartz thermometer with an accuracy of about 0.02 K. The inaccuracy in temperature measurements due to calibration errors of the thermocouples may lead to a deviation of approximately ±0.2 K. The pressure of the system was measured with strain-gauge sensors having a factory calibration of about 0.5% of the operating range, which was adequate for the experimental measurements.

3. Experimental results and discussion

3.1. Effect of heat flux and fluid velocity

Figs. 3a and 3b show typical measured flow boiling heat transfer coefficients as a function of heat flux for pure acetone and for a ternary mixture of acetone, isopropanol and water, respectively, over a wide range of fluid velocity. Two distinct regimes can be observed:

1. At low heat fluxes, heat transfer occurs by convection and the heat transfer coefficient is almost independent of the heat flux. The small increase of the heat transfer coefficient with heat flux is due to superimposed natural convection currents and due to changes in the physical properties of the fluids, both as a result of the increased wall superheat. Natural convection is a result of density differences and is, therefore, most prominent at higher heat fluxes and low velocities.

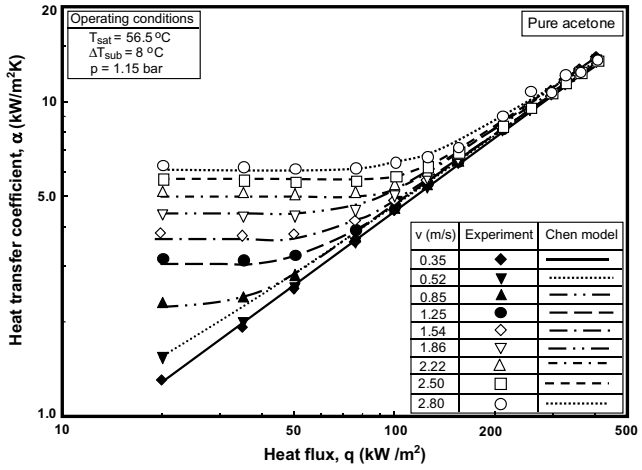

Fig. 3a. Heat transfer coefficient as a function of heat flux for pure acetone.

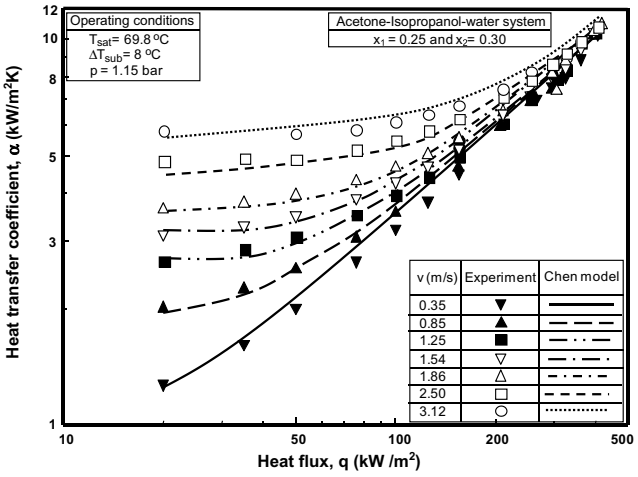

Fig. 3b. Heat transfer coefficient as a function of heat flux for a typical ternary mixture.

2. At moderate heat fluxes, the wall superheat leads to the formation of bubbles at the heat transfer surface. When boiling has been initiated, only few nucleation sites are operating and a significant proportion of the heat will still be transferred by forced convection. The number of active nucleation sites increases with increasing heat flux, improving the heat transfer coefficient because the bubbles disturb the laminar sublayer (see Fig. 4). Fully developed boiling is reached once the total heat transfer surface is covered with bubbles and the forced convection contribution is reduced to low values. For developed boiling, the influence of heat flux is strong, while flow velocity has little or no effect on the surface temperature and, therefore, the heat transfer coefficient. Nucleate boiling is now the dominant mechanism and all experimental data converge into a single line even though the flow velocity is varied from 0.3 to 3 m/s.

3.2. Effects of fluid composition and subcooling

Typical effects of composition on the heat transfer coefficient are shown in Fig. 5 where the heat transfer coefficient for mixtures of acetone and isopropanol are presented as a function of the composition of acetone, which is the more volatile component, over a wide range of heat fluxes. The highest heat transfer coefficient was recorded for pure components at all heat fluxes. A small addition of acetone to pure isopropanol causes the heat transfer coefficient to decrease sharply. Further addition causes a further reduction down to a minimum value, beyond which the transfer coefficient gradually increases again towards the value of the more volatile component. Similar trends have also been observed for other binary mixtures. Fig. 6 is a three-dimensional representation of the measured heat transfer coefficients for the ternary system acetone/isopropanol/water for constant values of subcooling, flow velocity, pressure and heat flux. Each point in

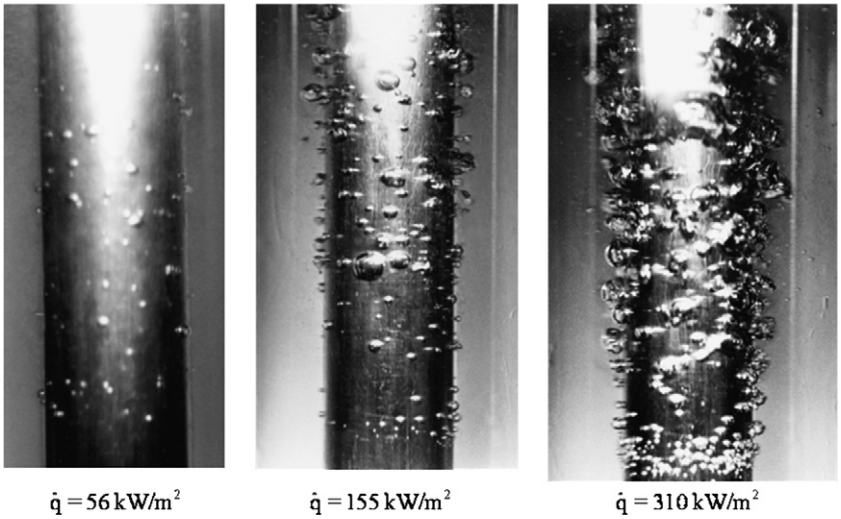

Fig. 4. Bubble formation for pure water at various heat fluxes ($v = 0.7$ m/s and $\Delta T_{sub} = 5$ °C).

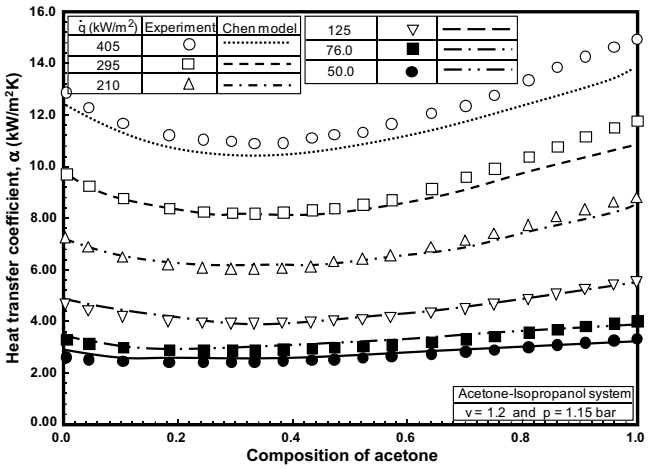

Fig. 5. Heat transfer coefficient as a function of acetone composition for several heat fluxes.

this triangular diagram represents the heat transfer coefficient of a specific ternary mixture, the outer corners of this surface stand for the heat transfer coefficients of the three pure components and, the outer border lines for the heat transfer coefficients of the corresponding binary mixtures.

Almost all investigators agree that the measured reduction of the heat transfer coefficient observed for liquid mixtures is caused by the liquid-side mass transfer resistance. The preferential evaporation of the more volatile component causes the liquid at the heat transfer surface to become depleted of the component with the higher vapor pressure, which results in an increase in the saturation temperature at the vapor–liquid interface. If the heat transfer coefficient is defined with the difference between wall temperature and bulk saturation temperature, this leads to a reduction in the measured value.

The effect of subcooling on the heat transfer coefficient is depicted in Fig. 7 for a typical ternary mixture. Subcool-

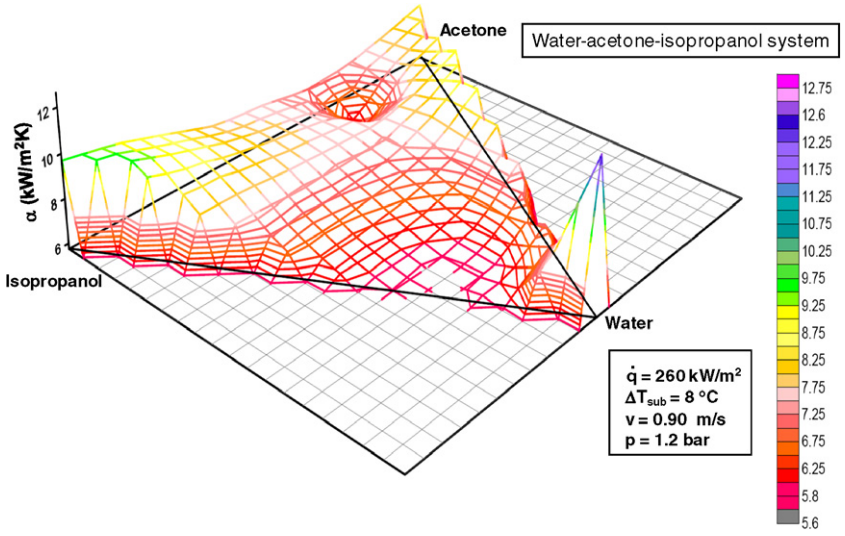

Fig. 6. Ternary diagram showing the variation of heat transfer coefficient with composition.

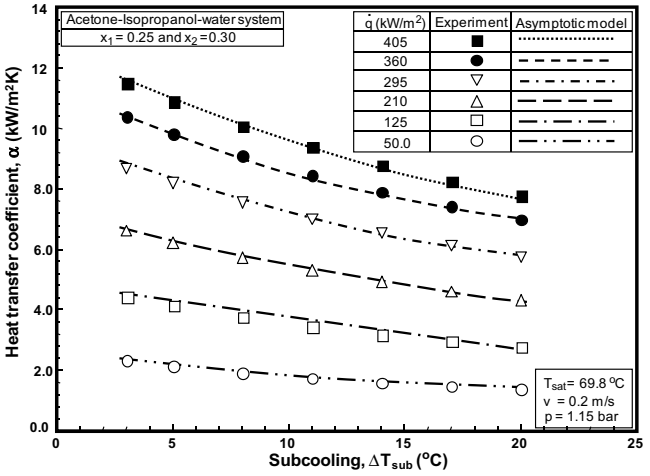

Fig. 7. Heat transfer coefficient as a function of subcooling for a typical ternary system.

ing is defined as the difference between the saturation temperature of the mixture and the bulk temperature, under the given conditions. The results indicate that the heat transfer coefficient decreases gradually as subcooling increases. This trend is explained by the fact the nominator in Eq. (2) can also be written as $[(T_w - T_{sat}) + (T_{sat} - T_b)]$ and that the second term varies more strongly with subcooling than the first. Indeed, the effect of subcooling on bubble growth mechanisms and hence $(T_w - T_{sat})$ is complex and depends strongly on composition and heat flux. This is discussed in more detail by Wenzel et al. [14]. For low heat fluxes, the contribution of forced convection dominates the total heat transfer and the effect of bulk temperature, i.e. subcooling, becomes less important.

4. Correlation of experimental data

4.1. Chen type model

It is generally believed that the heat transfer coefficient during flow boiling is affected by the interaction of nucleate boiling and forced convective heat transfer mechanisms. The first model to correlate flow boiling by combining nucleate boiling and forced convective heat transfer coefficients was suggested by Rohsenow [15] in form of a simple addition of the two coefficients:

$$\alpha_{fb} = \alpha_{pb} + \alpha_{fc} \tag{6}$$

Chen [10] refined Eq. (6) to develop a model that has long been considered one of the best available correlations for pure fluids under saturated and subcooled flow conditions. The Chen model in its basic form is expressed as:

$$\alpha_{fb} = \alpha_{fc} \cdot F + \alpha_{pb} \cdot S \tag{7}$$

In terms of heat flux, Eq. (7) becomes:

$$\dot{q} = \alpha_{fc}(T_w - T_b) \cdot F + \alpha_{pb}(T_w - T_{sat}) \cdot S = \dot{q}_{fc} \cdot F + \dot{q}_{pb} S \tag{8}$$

where α_{fc} is the convective heat transfer coefficient that would be found for the liquid phase flowing alone. The parameter F is a multiplier that accounts for the apparent increase in velocity due to the presence of the vapor and is a function of the Martinelli parameter X_{tt}. α_{pb} is the pool boiling heat transfer coefficient at the local wall superheat. The "suppression factor" S accounts for the fact that α_{pb} is found from pool boiling correlations which over-predicts nucleate flow boiling. The original paper gave graphical correlations for F and S. Coiller [16] fitted the following equations to the graphical relationships for F and S:

$$F = \begin{cases} 1 & \text{if } \frac{1}{X_{tt}} \leqslant 0.1 \\ 2.35\left(\frac{1}{X_{tt}} + 0.213\right)^{0.736} & \text{for } \frac{1}{X_{tt}} \geqslant 0.1 \end{cases} \quad \text{and}$$

$$S = \frac{1}{1 + 2.53 \times 10^{-6} Re_{tp}^{1.17}} \tag{9}$$

where

$$X_{tt} = \left(\frac{1-\dot{x}}{\dot{x}}\right)^{0.9} \left(\frac{\rho_v}{\rho_l}\right)^{0.5} \left(\frac{\mu_l}{\mu_v}\right)^{0.1} \quad \text{and}$$

$$Re_{tp} = \frac{\dot{m}(1-\dot{x})d_h}{\mu_l} F^{1.25} \tag{10}$$

Subsequently, Bennett and Chen [17] modified the original Chen correlation for mixtures, by using experimental data obtained for mixtures of water and glycol. Celata et al. [18] compared their experimental data for boiling of refrigerant mixtures with the prediction of both, the Chen [10] and the Bennett and Chen [17] correlations. They found that the performance of the correlation for pure fluids was almost the same as that for mixtures, with an error greater than ±20%.

To calculate the enhancement and suppression factors according to Eqs. (9) and (10), the local vapor mass fraction has to be known. Schröder [19] presented a calculation procedure for the local vapor mass fraction, which is applicable for subcooled and saturated boiling:

$$\dot{x} = Ph - Ph_n \exp\left(\frac{Ph}{Ph_n} - 1\right) \tag{11}$$

where Ph is the phase change number and is defined as:

$$Ph = \frac{h_v - h_{l,sat}}{\Delta h_v} \tag{12}$$

where Ph_n is the value of the phase change number which is reached once the mean fluid temperature is high enough to permit the existence of vapor bubbles in the bulk of the liquid. Schröder [19] suggested to calculate Ph_n with a correlation valid for laminar and turbulent flow using the boiling number Bo and the Peclet number Pe:

$$Ph_n = \frac{-Bo}{\sqrt{\left(\frac{455}{Pe_l}\right)^2 + 0.0065^2}} \quad \text{with}$$

$$Bo = \frac{\dot{q}}{\dot{m}\Delta h_v} \quad \text{and} \quad Pe = \frac{\dot{m} c_p d_h}{\lambda} \tag{13}$$

The length from the beginning of the test section to the point where the phase change number is zero is calculated from Eqs. (14) and (15) as:

$$\Delta L = \frac{-Ph_o d_h}{4Bo} \tag{14}$$

where

$$Ph_o = \frac{-c_{pl}(T_{sat} - T_b)}{\Delta h_v} \tag{15}$$

From Eq. (15) the phase change number at the beginning of the heated section can be calculated which gives the characteristic length ΔL from Eq. (14). From ΔL the length coordinate for the actual thermocouple position can be calculated:

$$\Delta L_t = \Delta L - x_{th} \tag{16}$$

With this length, the phase change number at the thermocouple location is:

$$Ph = \frac{-4Bo\Delta L_t}{d_h} \tag{17}$$

The Chen model also requires both forced convective and nucleate boiling heat transfer coefficients.

4.2. Force convective heat transfer

In his original work, Chen [10] used the Dittus–Bolter [20] correlation to calculate the turbulent convective heat transfer coefficient to the liquid. Jamialahmadi and Müller-Steinhagen [21] proposed a different approach since more reliable correlations for convective heat transfer have become available. A superposition of laminar and turbulent heat transfer coefficients is used for Reynolds numbers below 10,000; for higher Reynolds numbers only the turbulent heat transfer coefficient is considered:

$$\alpha_{fc} = \begin{cases} \sqrt[3]{\alpha_{lam}^3 + \alpha_{turb}^3} & \text{for } Re \leqslant 10,000 \\ \alpha_{turb} & \text{for } Re \geqslant 10,000 \end{cases} \tag{18}$$

The laminar heat transfer coefficient for flow in annuli is calculated by a superposition of the Nusselt numbers for fully developed and for developing flow as recommended in the VDI-Wärmeatlas [22]:

$$\alpha_{lam} = \left(Nu_{q,1}^3 + (Nu_{q,2} - 1)^3 + Nu_{q,3}^3\right)^{\frac{1}{3}} \cdot \left(\frac{Pr_b}{Pr_w}\right)^{0.11} \tag{19}$$

where

$$Nu_{q,1} = 4.364 \quad \text{and} \quad Nu_{q,2} = 1.302\left(Re \cdot Pr\frac{d_h}{L}\right)^{\frac{1}{3}} \tag{20}$$

and

$$Nu_{q,3} = 0.462 Pr^{\frac{1}{3}}\left(Re\frac{d_h}{L}\right)^{\frac{1}{2}} \tag{21}$$

To calculate the turbulent heat transfer coefficient in Eq. (19), the correlation suggested by Gnielinski [23] for the turbulent regime in annuli is used:

$$Nu_{turb} = 0.86\left(\frac{d_i}{d_o}\right)^{-0.16}\left(\frac{\frac{f}{2}RePr}{1 + 12.7\sqrt{\frac{f}{8}}\left(Pr^{\frac{2}{3}} - 1\right)}\right) \times \left(1 + \left(\frac{d_h}{L}\right)^{\frac{2}{3}}\right) \cdot \left(\frac{Pr_b}{Pr_w}\right)^{0.11} \tag{22}$$

The friction factor for turbulent flow in technically smooth pipes is calculated according to Filonenko [24]:

$$f = (1.82\log_{10}Re - 1.64)^{-2} \tag{23}$$

While the contribution of natural convection is usually small it can easily be incorporated into the correlation if the Reynolds number is calculated following a recommendation by Schlünder [25]:

$$Re = \sqrt{Re_f^2 + \frac{Gr}{2.5}} \tag{24}$$

where Re_f and Gr are the forced convection Reynolds number and the Grashof number, respectively. Excellent agreement between measured data and the predictions of the Gnielinski model has been reported for electrolytic solutions [21], pure hydrocarbons and for liquid mixtures [26]. Similar equations are given in the VDI-Wärmeatlas [22] for flow in cylindrical pipes.

4.3. Nucleate boiling heat transfer

4.3.1. Pure fluids

One of the most reliable pool boiling correlations for pure fluids was developed by Gorenflo [27]. This model reads:

$$\frac{\alpha}{\alpha_0} = F_q \cdot F_p \cdot F_{WR} \cdot F_{WM} \tag{25}$$

where

$$F_q = (q/q_0)^n, \quad n = 0.9 - 0.3p_r^a \tag{26}$$

The parameter a is equal to 0.3 for organic liquids and 0.15 for water and low boiling point liquids.

$$F_p = 1.2p_r^{0.27} + 2.5p_r + \frac{p_r}{1 - p_r} \tag{27}$$

and

$$F_{WR} = \left(\frac{R_p}{R_{p0}}\right)^{2/15} \quad \text{and} \quad F_{WM} = \left(\frac{\lambda\rho c_p}{\lambda_0\rho_0 c_{p0}}\right)^{1/4} \tag{28}$$

Values of the reference heat transfer coefficient α_0 for a reference heat flux of $q_0 = 20\ \text{kW/m}^2$ and the surface roughness R_{p0} are given by Gorenflo [27].

4.3.2. Liquid mixtures

The boiling heat transfer coefficient of liquid mixtures is a function of heat flux and liquid composition. Because of

the preferential evaporation of the more volatile component, the liquid-side mass transfer resistance results in a higher saturation temperature at the vapor/liquid interface than for bulk composition. Schlünder [25] used this interfacial saturation temperature to correlate the nucleate boiling heat transfer coefficient of mixtures:

$$\frac{\alpha_{pb}}{\alpha_{id}} = \left(1 + \frac{\alpha_{id}}{\dot{q}}(T_{ph} - T_{sat})\right)^{-1} \tag{29}$$

The ideal heat transfer coefficient α_{id} may be considered as the heat transfer coefficient of a hypothetical fluid with the same physical properties as the solution, but without any kinetic mixing effect. For pool boiling of mixtures, it frequently defined as:

$$\frac{1}{\alpha_{id}} = \sum_{j=1}^{n} \frac{x_j}{\alpha_j} \tag{30}$$

where α_j represents the heat transfer coefficient of the pure components at the same heat flux as the mixture. The interfacial temperature T_{ph} is a function of the interfacial composition of liquid and vapor phases. Gropp and Schlünder [28] by assuming that the heat transfer area is equal to the area for mass transfer have shown that:

$$\frac{y_{i,ph} - x_i}{y_{i,ph} - x_{i,ph}} = \exp\left(\frac{-\dot{q}_{boil}}{\rho_l \beta_l \Delta h_v}\right) = \exp(-\xi) \text{ where}$$

$$\xi = \frac{\dot{q}_{boil}}{\rho_l \beta_l \Delta h_v} \tag{31}$$

Eq. (31) gives the relationship between the interfacial composition, liquid side mass transfer coefficient and boiling heat flux. This equation can be solved by iteration to give the liquid concentration of each component at the interface. The vapor–liquid equilibria required for this calculation can be obtained using the Antoine equations for the vapor pressures and the Wilson equations for the activity coefficients, i.e. Eqs. (3)–(5). Different approaches to determine the liquid-side mass transfer coefficients using the Stefan–Maxwell equations have been evaluated [26] but did not provide any improvement over the use of a constant value of 0.5×10^{-4} m/s.

Heat transfer coefficients calculated from Eq. (29) are for saturated pool boiling and based on the difference between wall and saturation temperature. To apply these values in Eq. (7) for subcooled flow boiling, they have to be recalculated according to Wenzel and Müller-Steinhagen [26]:

$$\alpha_{sub} = \alpha_{pb}\left(\frac{T_w - T_{sat}}{T_w - T_b}\right) \tag{32}$$

The above models and equations have been compiled in a computer code for the calculation of subcooled flow boiling of single and multi-component mixtures. The flow chart of these calculations is given in Fig. 8. The input data are heat flux, fluid composition, temperature, fluid velocity and pressure. To start the calculation, the program requires the wall temperature T_w, which is initially not known for constant heat flux boundary conditions. Therefore, a trial and error procedure is adapted. The other steps of the program are summarized in the flow chart of the program. The outputs of the program are the wall temperature, heat transfer coefficient and the fraction of heat which is transferred by nucleate boiling:

$$\text{NBF} = \frac{\alpha_{sub} \cdot S}{\alpha_{fb}} \tag{33}$$

This parameter may be interpreted as a measure of the fraction of the heat transfer area affected by bubble growth mechanisms. The predicted heat transfer coefficients have also been included in Figs. 3a and 3b for pure fluids and mixtures over a wide range of fluid velocity, heat flux and composition. The results show that the agreement between measured and predicted heat transfer coefficients is acceptable. A comparison between all measured and predicted heat transfer coefficients for the entire range of the present investigations is given in Fig. 9. The narrow distribution of the points indicates that the described Chen type model predicts the flow boiling heat transfer coefficient reasonably well. The absolute mean average error between model and experimental data are about 15%.

4.4. Generalized asymptotic model

Many correlations for flow boiling recommended in the literature are based on the general relationship suggested by Kutateladze [29]:

$$\alpha_{fb} = \left[\alpha_{fc}^n + \alpha_{pb}^n\right]^{\frac{1}{n}} \tag{34}$$

Eq. (34) is termed asymptotic model because the value of α_{fb} approaches the larger of the two components α_{fc} and α_{pb}. This guarantees a smooth transition as the boiling mechanism changes with increasing heat flux from forced convection to nucleate boiling. As discussed before, Rohsenow [15] recommended $n = 1$, and the Chen model was a modification of this additive model by introducing flow boiling correction factor and nucleate boiling suppression factor. Contrariwise, Kutateladze [29] suggested an exponent $n = 2$.

Heat transfer coefficients calculated from Eq. (34) are for saturated boiling which is based on the difference between wall temperature and saturation temperature:

$$\alpha_{fb} = \frac{\dot{q}}{T_w - T_{sat}} \tag{35}$$

For subcooled flow boiling the heat transfer coefficient is defined as

$$\alpha_{sub} = \frac{\dot{q}}{T_w - T_b} \tag{36}$$

Combination of Eqs. (35) and (36) yields:

$$\alpha_{sub} = \left[\frac{1}{\alpha_{fb}} - \frac{T_{sat} - T_b}{\dot{q}}\right]^{-1} \tag{37}$$

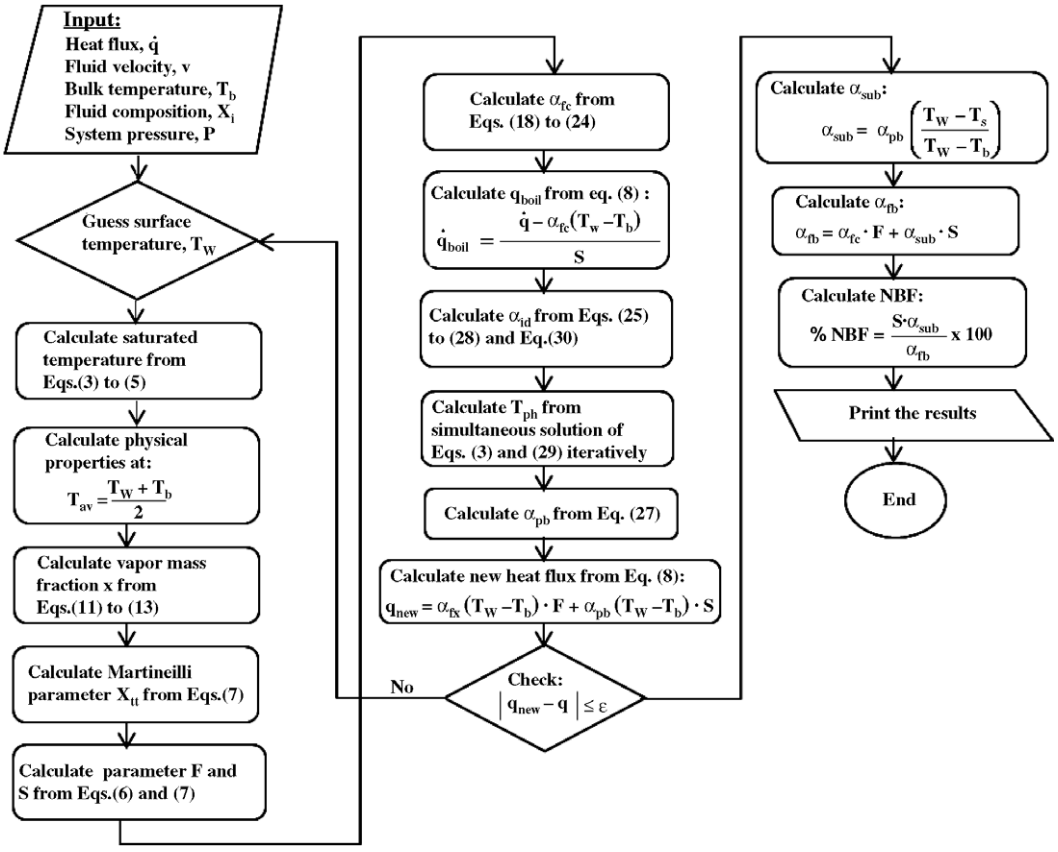

Fig. 8. Flowchart of the Chen type model.

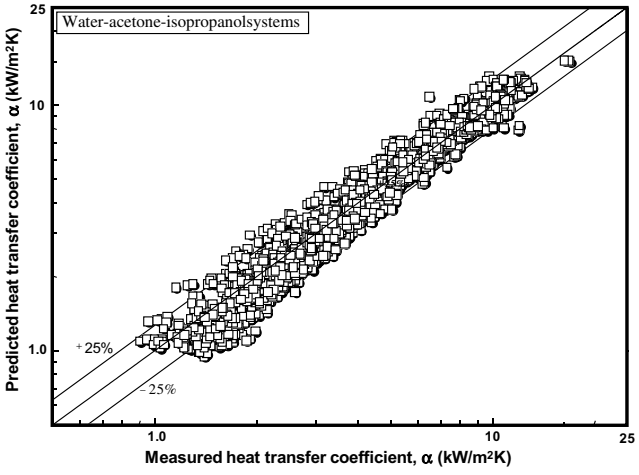

Fig. 9. Comparison of measured heat transfer coefficients with values calculated from the Chen type model.

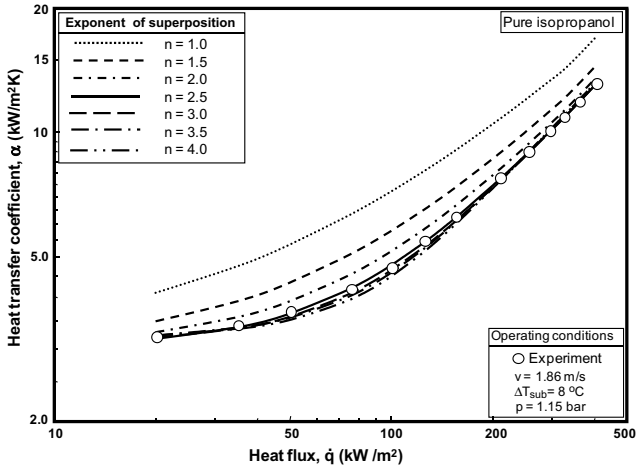

Fig. 10. Effect of value of exponent *n* in the asymptotic model on the flow boiling heat transfer coefficient.

Fig. 10 shows the flow boiling heat transfer coefficient as a function of heat flux for different values of the exponent n, indicating that as the value of *n* increases, the prediction of Eq. (34) improves and approaches the experimental values. The prediction of flow boiling heat transfer is only slightly affected by increasing the value of *n* further than 3. The absolute mean average error of all the experimental data are plotted against the value of *n* in Fig. 11. The results show that changing the value of exponent *n* from 1 to 2 is accompanied by a sharp reduction in the percentage of error. If *n* is increased further, the average error decreases gradually and reaches a minimum value of about 8% for the asymptotic model with exponent 2.5. After this point the error stabilizes and very gradually deteriorates again. For comparison, the error of the Chen model, which is about 15%, is also included in Fig. 11. The advantages of

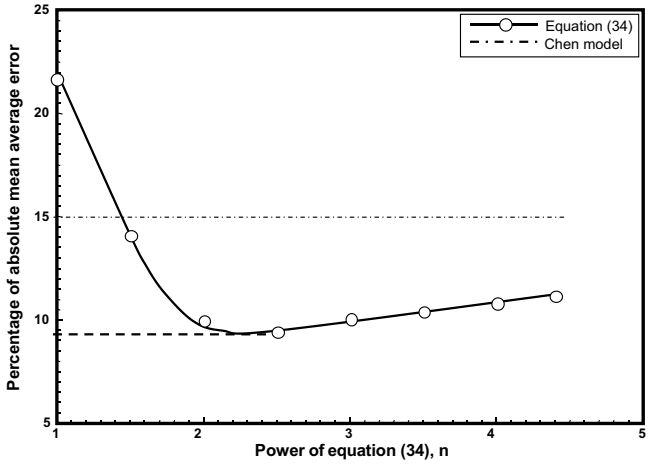

Fig. 11. The effect of superposition exponent n on the accuracy of the asymptotic model.

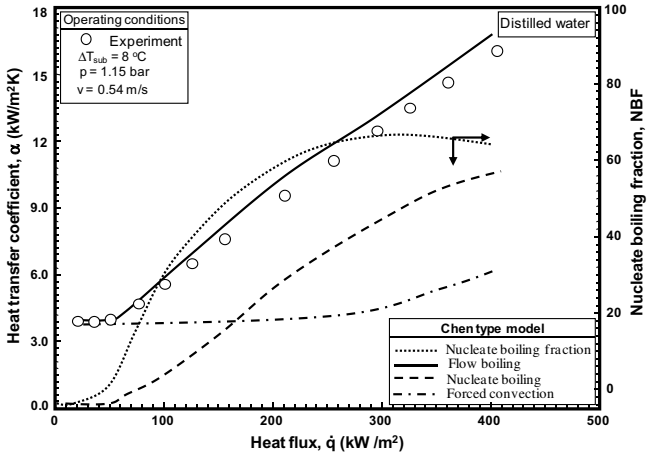

Fig. 12a. Contribution of forced convective and nucleate boiling heat transfer coefficients according to the Chen model.

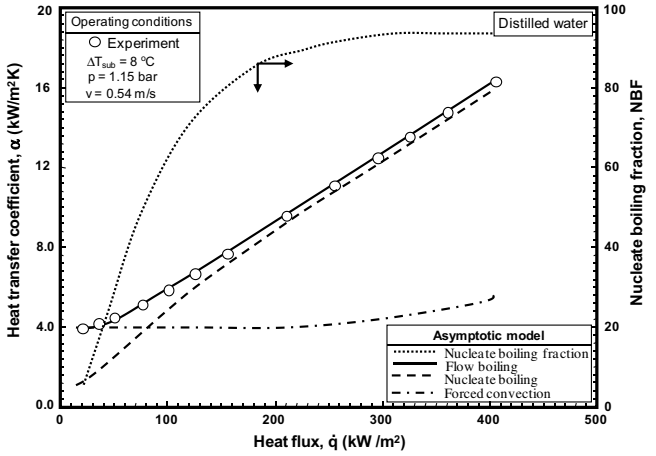

Fig. 12b. Contributions of forced convective and nucleate boiling heat transfer coefficients according to the asymptotic model.

the asymptotic model are its simplicity and non-iterative nature in comparison to the Chen type model, because in this model Eqs. (8)–(17) are eliminated. These simplifications make the calculations of flow boiling heat transfer coefficient very simple and fast.

4.5. Nucleate boiling fraction

Many, if not most, industrial boilers suffer from the formation of process-related deposits, i.e. fouling, on the heat transfer surfaces. The rapid evaporation at the base of bubbles leads to local supersaturation conditions, and hence the precipitation of dissolved materials on the area of the heat transfer surface affected by bubble formation. Hence, the relative contribution of nucleate boiling heat transfer to the total heat transfer (i.e. the nucleate boiling fraction NBF) is of crucial importance for the prediction of fouling rates and the resulting design of heat exchangers. Prediction methods for the contributions of the different boiling mechanisms toward the total amount of heat transferred can be found in Piening [30] and Najibi et al. [31].

Figs. 12a and 12b show the heat transfer coefficients for forced convection α_{fc}, nucleate boiling α_{pb}, flow boiling α_{fb} and the nucleate boiling fraction NBF as a function of heat flux for distilled water, as predicted from the Chen type and asymptotic model, respectively. Similar trends are also obtained for pure acetone, pure isopropanol as well as for the ternary mixtures.

Fig. 12a shows a significant weakness of the Chen type model which puts its physical correctness into question. For pure water this model predicts that there are no active nucleation sites on the heat transfer surface for heat fluxes below 100 kW/m^2, and that forced convective heat transfer is the dominant mechanism over the entire surface. Contrariwise, visual observations for these conditions show a significant number of active nucleation sites on the heat transfer surface, see Fig. 4. As illustrated in Fig. 12a, the Chen model never reaches the fully developed boiling regime. As the heat flux is increased from 0 to 300 kW/m^2, the contribution of nucleate boiling increases gradually up to about 65%, while the contribution of forced convection almost remains constant. Further increase of the heat flux causes the contribution of forced convective to rise and nucleate boiling to decline. The experimental results show, however, that at these heat fluxes the entire heat transfer surface is densely covered with vapor bubbles and that the influence of flow velocity becomes insignificant, i.e. nucleate boiling is the dominant heat transfer mechanism (see Figs. 3a and 3b). In some cases, such as for pure water, strict application of the Chen model even leads to negative values for nucleate boiling. This discrepancy must be associated with the calculation of the values of the parameters S and F.

Contrary to this, the asymptotic model shows that for heat fluxes below 70 kW/m^2, the nucleate boiling heat transfer is negligible compared to forced convective heat transfer. At moderate heat fluxes (70–200 kW/m^2) both mechanisms are important and at high heat fluxes, nucleate

boiling heat transfer is the dominate mechanism. The nucleate boiling fraction levels-off at values above 90%, which seems to be a reasonable value considering the appearance of the heat transfer surface under these conditions.

Hence, the advantage of the asymptotic model in comparison to the Chen type model is not only its simplicity and the more accurate prediction of flow boiling heat transfer coefficients, but most likely also the physically sounder prediction of the nucleate boiling fraction NBF. Based on these findings, the fouling model suggested by Najibi et al. [31] will now be re-evaluated against previous and more recent experimental data, to improve its accuracy of prediction.

5. Conclusions

Subcooled flow boiling heat transfer coefficients for pure, binary and ternary mixtures of acetone, isopropanol and distilled water have been measured over a wide range of flow velocity, composition, subcooling and heat flux. Two models, namely a Chen type model and an asymptotic model, are presented to predict flow boiling heat transfer coefficient and nucleate boiling fraction NBF for single component liquids and mixtures. Both models are applicable for saturated and subcooled conditions covering the regimes of convective, transition and fully developed flow boiling heat transfer. Comparison with a large number of experimental data shows that the Chen type model predicts the heat transfer coefficients satisfactory but fails with respect to the prediction of nucleate boiling fraction NBF. On the other hand, the asymptotic model predicts the heat transfer coefficients and the nucleate boiling fraction with good accuracy.

References

[1] U. Wenzel, Saturated pool boiling and subcooled flow boiling of mixtures at atmospheric pressure, Ph.D. Thesis, University of Auckland, Auckland, New Zealand, 1992.
[2] L.S. Tong, Boiling Heat Transfer and Two-Phase Flow, Robert E. Krieger Publishing Company, Huntington, New York, 1975.
[3] M. Jamialahmadi, R. Blöchl, H. Müller-Steinhagen, Pool boiling heat transfer to saturated water and Refrigerant 113, Can. J. Chem. Eng. 69 (1991) 746–753.
[4] M. Jamialahmadi, R. Blöchl, H. Müller-Steinhagen, Bubble dynamics and scale formation during boiling of aqueous calcium sulfate solutions, Chem. Eng. Process. 26 (1989) 15–26.
[5] D. Steiner, J. Taborek, Flow boiling heat transfer in vertical tubes correlated by an asymptotic model, Heat Transfer Eng. 13 (1992) 43–69.
[6] J.R. Thome, Boiling of new refrigerants: a state-of-the-art review, Int. J. Refrig. 19 (1996) 435–457.
[7] S.G. Kandlikar, Boiling heat transfer with binary mixtures: Part II – flow boiling in plain tubes, J. Heat Transfer 120 (1998) 388–394.
[8] K. Stephan, Two-phase heat exchange for new refrigerants and their mixtures, Int. J. Refrig. 18 (1995) 198–209.
[9] L. Cheng, D. Mewes, Review of two-phase flow and flow boiling of mixtures in small and mini channels, Int. J. Multiphase Flow 32 (2006) 183–207.
[10] J.C. Chen, A correlation for boiling heat transfer to saturated fluid in vertical flow, Ind. Eng. Chem. Proc. Design Dev. 5 (1966) 322–329.
[11] A. Helalizadeh, Mixed salt crystallization fouling, Ph.D. Thesis, University of Surrey, Guildford, UK, 2002.
[12] V. Gnielinski, New equations for heat and mass transfer in turbulent pipe and channel flow, Int. Chem. Eng. 16 (1976) 359–368.
[13] M. Müller-Steinhagen, A.P. Watkinson, N. Epstein, Subcooled boiling and convective heat transfer to heptane flowing inside an annulus and past a coiled wire, J. Heat Transfer 108 (1986) 922–933.
[14] U. Wenzel, B. Hartmuth, H. Müller-Steinhagen, Heat transfer to mixtures of acetone, isopropanol and water under subcooled flow boiling conditions – 1. Experimental results, Int. J. Heat Mass Transfer 37 (1994) 175–183.
[15] W.M. Rohsenow, Chapter in Heat Transfer, University of Michigan Press, Ann Arbor, IL, 1953.
[16] J.G. Coiller, Boiling within vertical tubes, Heat Exchanger Design Handbook, Fluid Mechanics and Heat Transfer, vol. 2, Hemisphere, Washington, DC, 1984.
[17] D.L. Bennett, J.C. Chen, Forced convective boiling in vertical tubes for saturated pure components and binary mixtures, AIChE J. 21 (1980) 454–461.
[18] G.P. Celata, M. Cumo, T. Setaro, Forced convective boiling in binary mixtures, Int. J. Heat Transfer 36 (1993) 3299–3309.
[19] J.J. Schröder, Heat Transfer During Subcooled Boiling, fifth ed., VDI-Wärmeatlas, 1988.
[20] F.W. Dittus, L.M.K. Bolter, Heat Transfer in Automobile Radiators of the Tubular Type, University of California Press, Berkeley, CA, 1930, pp. 13–18.
[21] M. Jamialahmadi, H. Müller-Steinhagen, Forced convective and subcooled flow boiling heat transfer to spent Bayer liquor, Light Met. (1992) 141–151.
[22] Wärmeübertragung in Rohren, VDI-Wämeatlas, sixth ed., VDI-Verlag, Düsseldof, 2002.
[23] V. Gnielinski, Wärmeübertragung in Rohren, VDI-Wämeatlas, sixth ed., VDI-Verlag, Düsseldof, 2002.
[24] G.K. Filonenko, Hydraulic resistance in pipes, Teploenergetika 1 (1954) 40–44.
[25] E.U. Schlünder, Einführung in die Lehre von der Wärmeübertragung, fourth ed., VDI-Wärmeatlas, Section A, 1984.
[26] U. Wenzel, H. Müller-Steinhagen, Heat transfer to mixtures of acetone, isopropanol and water under subcooled flow boiling conditions – II. Prediction of heat transfer coefficients, Int. J. Heat Mass Transfer 17 (1994) 185–194.
[27] D. Gorenflo, Behältersieden, VDI-Wärmeatlas, Sec Ha, sixth ed., VDI-Düsseldorf, 2002.
[28] U. Gropp, E.U. Schlünder, The influence of liquid side mass transfer on heat transfer and selectivity during surface and nucleate boiling of liquid mixtures in a falling film, Chem. Eng. Process. 20 (1986) 103–114.
[29] S.S. Kutateladze, Boiling heat transfer, J. Heat Mass Transfer 4 (1961) 31–45.
[30] J. Piening, Wärmeübergang an einer an der Heizwand wachsenden Dampfblase beim Sieden, Ph.D. Thesis, TU Berlin, Germany, 1971.
[31] S.H. Najibi, H. Müller-Steinhagen, M. Jamialahmadi, Calcium sulfate scale formation during subcooled flow boiling, Chem. Eng. Sci. 52 (1997) 1265–1284.